The Phase Transition of Nematic Liquid Crystal Cells Bounded by Surfactant-Laden Interfaces

The Phase Transition of Nematic Liquid Crystal Cells Bounded by Surfactant-Laden Interfaces *

ZENG Ming-Ying(曾明颖)[1,2], CUI Wei(崔伟)[1], TAN Xiao-Qin(谭晓琴)[1], WU Chen-Xu(吴晨旭)[1**]

[1]*Department of Physics and ITPA, Xiamen University, Xiamen 361005*
[2]*College of Information Science and Engineering, Huaqiao University, Xiamen 361021*

Taking into account the surface-coupling strength effect, we discuss the phase transitions of a finite thickness cell bounded by surfactant-laden interfaces in a magnetic field perpendicular to the substrate and it is compared with that of a semi-infinite system. It is found that the larger the thickness, the closer the three-dimensional phase transition surface of the finite system to that of the semi-infinite one. The simulation also shows that when a magnetic field is applied to a nematic semi-infinite sample, an orientational phase transition first takes place close to the interface and then extends to the inner space as the temperature increases.

Thermotropic liquid crystals at a surfactant-laden interface exhibit a large variety of phenomena related to wetting and anchoring.[1−4] One of the earliest works about wetting can be dated back as far as 1970s when Sheng reported his important work on the phase transition of the surface-aligned nematic liquid crystals,[2,3] which did not include the application of an external field. Similar works can be found in Cahn's work on critical point wetting.[5,6] The study of surface-induced phenomena not only is of technological importance to potential applications but also provides a useful approach to probe the surface coupling effect.[7,8] So far, there have been lots of investigations, both theoretically and experimentally, in the literature about the anchoring states, which can be homeotropic, planar unidirectional or planar degenerate.[9] In nematic liquid crystals, molecular interactions are strong enough to create a long-range orientational order with rod-like molecules aligned, averagely, parallel to the director $n(n^2 = 1)$. It is widely known that nematic liquid crystals undergoe a nematic-isotropic phase transition in the absence of external field under certain environmental changes such as temperature. When an external field is applied, the isotropic phase becomes paranematic with large pretransitional effect,[10] and a field-induced paranematic-nematic transition occurs, as predicted by the Landau-de Gennes model.[11−13] Microscopically the Landau-de Gennes model also predicted a large variety of pretransitional wetting behaviors under the influence of the surface coupling effect.[14−16] Recently, using a simple quadratic surface free energy for nondegenerate ordering, Kadivar[17] systematically studied the phase transition of semi-infinite liquid crystal system in the presence of an external magnetic field. In this Letter, phase transitions in a liquid crystal cell in the presence of an external field are studied and analyzed by taking into account the

quadratic coupling between bulk and substrate, which induce many phenomena in surfactant-laden interfaces and are of technological importance. The comparison with those of a semi-finite system is also made, indicating the size effect of the liquid crystal cell.

To model a liquid crystal cell, we consider a system of uniform thickness $2D$ in which a nematic liquid crystal is sandwiched between two identically treated substrates situated at $z = 0$ and $z = 2D$, respectively. The system is applied by an external magnetic field h along the z axis. According to the Landau-de Gennes model, the free energy per unit area for the system in terms of the Maier–Saupe order parameter $S(z)$ [17] is given by

$$F_{\mathrm{A}}[S(z)] = 2 \int_0^D \Big[f_b + \Big(\frac{dS}{dz} \Big)^2 \Big] dz + 2\gamma [S_0 - S_S]^2, \quad (1)$$

with

$$f_b = tS^2 - \frac{1}{\sqrt{6}} S^3 + \frac{1}{3} S^4 - hS, \quad (2)$$

where f_b the bulk free energy density, t and h are the reduced temperature and the reduced magnetic field respectively. The second term in the integration describes the one-constant approximation of elastic energy penalizing any nonuniform orientational order distribution. The last term in Eq. (1) is a simple quadratic surface free energy accounting for nondegenerate ordering. Here S_0 is the order parameter on the planes $z = 0$ and $z = 2D$, S_s is the order parameter preferred by the substrate and γ is the reduced liquid crystal-surface coupling strength which is positive in the present study, indicating a cost of energy for any deviation from the anchoring direction preferred. Sheng[2,3] used a linear ordering rather than a quadratic disordering term and the connection between these two sets of calculations had been made by Poniewierski and Sluckin.[18,19]

A variation of the free energy Eq. (1) gives the

**Email: cxwu@xmu.edu.cn

Euler–Lagrange equation

$$\frac{d^2S}{d^2z} = \frac{1}{2}\frac{df_b}{dS}, \qquad (3)$$

which governs the equilibrium sates of bulk. The system is confined with two boundary conditions, that is, $dS/dz|_{z=0, z=2D} = \gamma[S_0 - S_S]$ at the interfaces and $dS/dz|_{z\to D} = 0$ or $\lim_{z\to D} S(z) = S_b$ at the middle of the sample. Here S_b is the order parameter in the middle of the system. Integrating Eq. (3) with consideration of the boundary conditions, one obtains

$$\left|\frac{dS}{dz}\right| = \sqrt{f_b(S) - f_b(S_b)}, \qquad (4)$$

Given Eqs. (3) and (4) as well as the boundary conditions, we have the correlation between bulk order and surface order

$$\gamma|S_0 - S_S| = \sqrt{f_b(S_0) - f_b(S_b)}, \qquad (5)$$

together with the free energy for the system

$$\frac{1}{2}F_A = f_b(S_b)D \pm 2\int_{S_0}^{S_b}\sqrt{f_b(S) - f_b(S_b)}dS + \gamma[S_0 - S_S]^2, \qquad (6)$$

where $f_b(S_b)D$ is the half bulk free energy when the whole liquid crystal cell, including the interfaces, exhibits the bulk order. When $dS/dz \geq 0$, the positive sign is taken, while $dS/dz \leq 0$ the negative sign is used.

A minimization of the free energy Eq. (6) yields

$$f_b'(S_b)\left[1 \mp \frac{1}{D}\int_{S_0}^{S_b}\frac{dS}{\sqrt{f_b(S) - f_b(S_b)}}\right] = 0, \qquad (7)$$

There are multiple pairs of solutions (S_0, S_b) and the appropriate pairs correspond to the lowest F_A given by Eq. (6). When $1/D \to 0$, Eq. (7) reduces to $f_b'(S_b) = 0$, the condition of lowest free energy for a semi-infinite system.

It is also clear that once S_0 is given to a liquid crystal cell, its orientational order profile $S(z)$,

$$z = \pm\int_{S_0}^{S(z)}\frac{dS}{\sqrt{f_b(S) - f_b(S_b)}}, \qquad (8)$$

can be obtained via an integration of Eq. (4).

In a liquid crystal cell, five parameters, i.e. h, $2D$, γ, t and S_s are important to determine the phase diagram. Given a thickness of the sample $2D$, an applied field h, a surface coupling strength γ and a temperature t (S_s is fixed at -0.3 in this study), the stable orientational orders of liquid crystal cell at the interfaces and bulk (S_0, S_b) corresponding to the lowest value of F_A given by Eq. (6) can be obtained.

The three-dimensional phase diagram with different sample thicknesses $2D$ is shown in Fig. 1(a). It

contains four critical curving surfaces as shown in Fig. 4(b). Each critical curving surface divides the parameter space into two regimes, one paranematic (left side) and one nematic (right side). It is found that in the finite-thickness sample the larger the sample thickness is, the closer the phase transition curve surface is to that of the bulk in the semi-infinite sample.
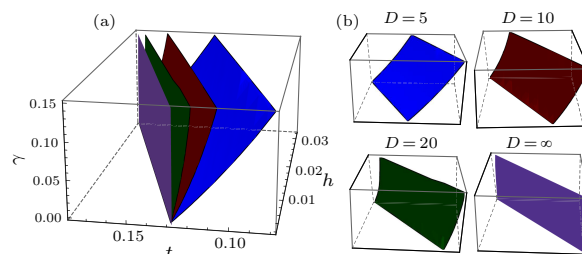
Fig. 1. Three-dimensional phase diagram of the finite sample with different thicknesses $2D = 10$, 20, 40 and of an infinite bulk respectively, dividing the parameter space into a paranematic phase (high-temperature regime) and a nematic one (low-temperature regime).
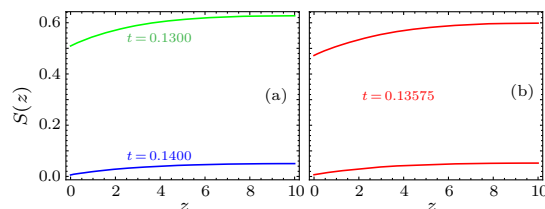

Fig. 2. (a) Order parameter S as a function of z when $D = 10$, $h = 0.012$, $\gamma = 0.050$ and $t = 0.1400$ (lower curve) and when $D = 10$, $h = 0.012$, $\gamma = 0.050$ and $t = 0.1300$ (upper curve). The liquid crystal at the interface and in the bulk are paranematic (lower curve) and nematic (upper curve) respectively. (b) Order parameter S as a function of z with $D = 10$, $h = 0.012$, $\gamma = 0.050$ and $t = 0.13575$, when the system is experiencing a phase transition from paranematic phase (lower curve) to nematic phase (upper curve).

To study the order parameter in this system, we plot its profile S as a function of z in Fig. 2 when the system is paranematic (lower curve, Fig. 2(a)), nematic (upper curve, Fig. 2(a)) or at a critical point (Fig. 2(b)). Despite the slight increase, the order parameter profiles do not change much with respect to location. It is also found that in a liquid crystal cell sandwiched by two interfacial layers, phase transition always occurs synchronously both close to the interfaces and in the bulk far from the interfaces (Fig. 2(b)).

In order to investigate the critical phenomena at constant external field, we take a look at the cross section of Fig. 1 by keeping $h = 0.016$ (Fig. 3(a)). The temperature at which phase transition occurs in the sample decreases with respect to the increasing surface coupling strength. Under the same surface coupling strength, the thicker the sample is, the higher the temperature at which the phase transition takes place is. The effect of the surface coupling makes less contribution in thicker samples and looks like saturated as the

thickness continues to increases. Similarly if we study the cross section of Fig. 1 at $\gamma = 0.050$ (Fig. 3(b)), a linear correlation is found between the transition temperature and the magnetic field applied. Each line separates the parameter space into two regimes, one paranematic and one nematic. The coexisting curves will approach to that of the bulk in semi-infinite sample[17] as the sample thickness continues to increase.
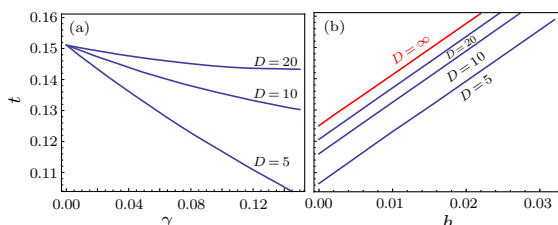
Fig. 3. (a) Phase transition temperature as a function of the surface coupling strength γ with different cell thicknesses for $h = 0.016$. (b) Phase transition temperature as a function of the magnetic field h with different cell thickness for $\gamma = 0.050$.

In the semi-infinite sample where the nematic liquid crystal is placed in the space $z > 0$ and bounded by a substrate situated at $z = 0$, the free energy per unit area for the system becomes[17]

$$F_A[S(z)] = \int_0^\infty \left[f_b + \left(\frac{dS}{dz} \right)^2 \right] dz + \gamma[S_0 - S_S]^2, \quad (9)$$

Similarly a variation of Eq. (9) together with boundary conditions $dS/dz|_{z=0} = \gamma[S_0 - S_S]$ at the interface and $dS/dz|_{z\to\infty} = 0$ or $\lim_{z\to\infty} S(z) = S_b$ far from the interface gives the minimum free energy

$$\begin{aligned} F_A = \int_0^\infty f_b(S_b)dS &\pm 2 \int_{S_0}^{S_b} \sqrt{f_b(S) - f_b(S_b)}dS \\ &+ \gamma[S_0 - S_S]^2, \end{aligned} \quad (10)$$

In the semi-infinite system, given a certain applied field h, the surface coupling strength γ and the temperature t, the bulk order S_b is obtained by minimizing f_b which is given by $f_b'(S_b) = 0$. S_0 can also be obtained once Eq. (5) is taken into account. Figure 4 shows the phase diagram for the semi-infinite sample using the Landau–Ginzburg theory. It is composed of one bulk branch for the LC molecules far from the substrate and one interface branch for the LC molecules close to the substrate, overlapping part of their coexisting surfaces (blue part of Fig. 4(c)) and dividing the parameter space into three regions. It is found that given a coupling strength, the larger the external magnetic field h is applied, the higher the phase transition temperature is achieved. The three-dimensional diagram of semi-infinite sample (Fig. 4(a)) also tells us that, unlike the liquid crystal molecules in bulk far from the substrate (Fig. 4(b)), the liquid crystal molecules close to the interface (Fig. 4(c)) can change from paranematic order to nematic order continuously

if the liquid crystal-surface coupling is large enough (above the green surface), indicating that a second or higher-order phase transition exists there. However, in the weak coupling regime, especially at high temperature and low field, the liquid crystal (either far from or close to the substrate) still prefers to make a first-order phase transition between paranematic order and nematic order.
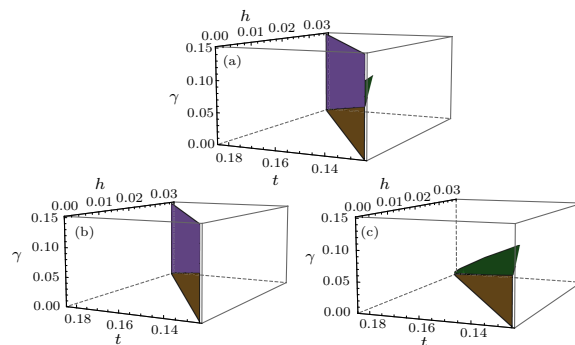
Fig. 4. Phase diagrams for (a) a semi-infinite system, which is composed of one bulk branch for (b) LC moelcules far from the substrate and one interface branch for (c) LC molecules close to the substrate, overlapping part (brown) of their coexisting surfaces.
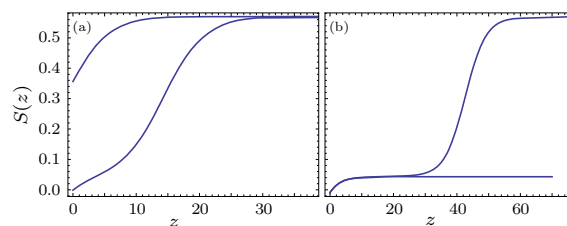
Fig. 5. (a) Order parameter $S(z)$ as a function of z with $h = 0.010$, $\gamma = 0.060$ and $t = 0.141$. A phase transition takes place close to the interface while the bulk remains to be nematic. (b) Order parameter $S(z)$ as a function of z with $h = 0.010$, $\gamma = 0.060$ and $t = 0.14133$. The liquid crystal in the bulk far from the substrate experiences a phase transition while the interface is paranematic.

A comparison between bulk branch (Fig. 4(b)) and interface branch (Fig. 4(c)) also reveals that the introduction of liquid crystal-surface coupling effect (with its strength $\gamma > 0$) does not change the bulk branch, but drives part of the coexisting interface branch to the higher temperature and field regime, making the region between the two coexisting surfaces a nematic phase for bulk molecules but a paranematic phase for LC molecules close to interface. This indicates that the liquid crystal-surface coupling favors paranematic structures. Given an external magnetic field, the liquid crystal on the surface experiences a phase transition at a decreasing critical temperature when the surface coupling is enhanced.

Figure 5 shows the order parameter profile $S(z)$ as a function of z in the semi-infinite system where a phase transition takes place close to the interface and in the bulk asynchronously.

In Fig. 5(a), a phase transition occurs at the inter-

face and the bulk remains to be nematic (the green part of Fig. 4(c)), while in Fig. 5(b), the liquid crystal in the bulk is undergoing a phase transition and the interface is still paranematic (the blue part of Fig. 4(b)). Thus inside a nematic semi-infinite sample, as the temperature increases, a phase transition from nematic to paranematic first takes place close to the interface and then extends to the inner space when an external magnetic field and the surface coupling strength are introduced. While in the low coupling regime (brown part), the phase transitions in the bulk far from substrate and close to the interface occur synchronously.

In a nematic semi-infinite system, phase transition takes place first close to the interface (green part, Fig. 5) and then propagates to the inner regime (blue part, Fig. 5), if the temperature increases and a moderate magnetic field and a moderate surface coupling are considered, while in a liquid crystal cell sandwiched by two interfacial layers phase transition always occurs synchronously both close to the interfaces and in the bulk far from the interfaces (Fig. 2(b)).
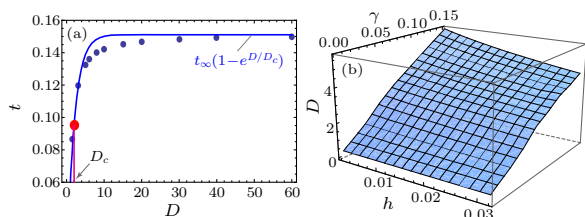
Fig. 6. (a)Phase transition temperature as a function of cell thickness while keeping $h = 0.016$ and $\gamma = 0.050$. Here D_C is the critical half thickness above which there is no difference between a semifinite system and a cell system. (b) Critical half thickness D_C versus h and γ.

The influence of controlled-pore glass confinement on the phase behavior of liquid crystal has been studied by Kralj *et al.* by means of x-ray scattering and high precision calorimetry.[20] For a liquid crystal cell sandwiched by interfaces, it is apparent that the phase transition temperature depends on cell thickness, as shown by dots in Fig. 6(a), where t_∞ is the phase transition temperature in the bulk of the semi-infinite system under the same magnetic field and surface coupling strength. The phase transition temperature increases dramatically against cell thickness in small thickness regime. As the cell thickness continues to increase, it levels off and saturates to the bulk's value of the infinite sample under the same magnetic field and the surface coupling strength. A fitting curve of exponential type is plotted on the basis of the dots,

giving a critical half cell thickness D_C of the system, beyond which the liquid crystal cell can be treated as a semi-infinite sample (Fig. 6(b)). It depends not only on the applied magnetic field h but also on the surface coupling strength γ.

In summary in the nematic semi-infinite sample, as the temperature increases, an orientational phase transition is found to first take place close to the interface and then extends to the inner space when a magnetic field is applied or a moderate surface coupling is taken into consideration. By taking into account the surface-coupling strength effect, the phase diagram of a finite thickness cell bounded by surfactant-laden interfaces in a magnetic field perpendicular to the substrate is obtained. The simulation shows that the larger the thickness, the closer the three dimensional phase transition surface of the finite system approaches to that of a semi-infinite one. In addition to the magnetic field dependence, one also sees the influence of surface coupling strength and cell thickness on critical temperature, indicating a possibility of controlling the critical behaviors of the system via the interface properties.

References

[1] de Gennes P G and Prost J 1993 *The Physics of Liquid Crystal*, 2nd ed (Oxford: Oxford Science Publications)
[2] Sheng P 1976 *Phys. Rev. Lett.* **37** 1059
[3] Sheng P 1982 *Phys. Rev.* A **26** 1610
[4] Fukuda J I, Stark H and Yokoyama H 2004 *Phys. Rev.* E **69** 021714
[5] Cahn J W 1977 *J. Chem. Phys.* **66** 3667
[6] Cahn J W 2000 *Physica* A **279** 195
[7] Jérôme B 1991 *Rep. Prog. Phys.* **54** 391
[8] Crawford G P, Ondris-Crawford R J, Doane J W and Žumer S 1996 *Phys. Rev.* E **53** 3647
[9] Sheng P and Wojtowicz P J 1976 *Phys. Rev.* A **14** 1883
[10] Zhao W, Wu C -X and Iwamoto M 2000 *Phys. Rev.* E **62** R1481-R1484
[11] Lelidis I, Nobili M and Durand G 1993 *Phys. Rev.* E **48** 3819
[12] Lelidis I and Durand G 1993 *Phys. Rev.* E **48** 3822
[13] Fan C and Stephen M 1970 *Phys. Rev. Lett.* **25** 500
[14] Telo Da Gama M M 1984 *Mol. Phys.* **52** 611
[15] Pawlowska Z, Sluckin T J and Kventsel G F 1988 *Phys. Rev.* A **38** 5342
[16] Somoza A M, Mederos L and Sullivan D E 1995 *Phys. Rev.* E **52** 5017
[17] Kadivar E 2008 *Phys. Rev.* E **78** 031706
[18] Poniewierskiab A and Sluckinac T J 1985 *Mol. Cryst. Liq. Cryst.* **126** 143
[19] Poniewierskiab A and Sluckinac T J 1987 *Liq. Cryst.* **2** 281
[20] Kralj S, Cordoyiannis G, Zidanšek A, Lahajnar G Amenitsch H, Žumer S and Kutnjak Z 2007 *J. Chem. Phys.* **127** 154905